A Novel Fractal Arrow-Shaped mmWave Flexible Antenna for IoT and 5G Communication Systems

Nazih K. Mallat[1, *], Alireza Jafarieh[2], Hamidreza Noorollahi[3], and Mahdi Nouri[2]

Abstract—In this paper, a novel flexible antenna for the new ISM band is proposed. A multi-objective optimization based on DDEA-SE is performed to optimize the antenna bandwidth and gain. The proposed optimized antenna has a 4 dB maximum realized gain and 50% maximum radiation efficiency on the ISM band. A fractal structure is used in this design to achieve a multi-band antenna. The bandwidth of this antenna covers several 5G bands. This multi-band antenna is fabricated on a cotton substrate. This antenna has a small dimension which makes it suitable for 5G applications. The bending tests are performed, and both simulation and measurement results show the good performance of the proposed antenna.

1. INTRODUCTION

The new applications of the fifth generation of mobile communication (5G) need a higher data rate, lower latency, and smaller size [1–3]. The available sub-6 GHz bandwidth (BW) is incapable to fulfill these demands [4]. Furthermore, 5G devices should have a small size. The vacant bandwidth of the millimeter wave (mmWave) spectrum seems to be capable to provide adequate bandwidth for 5G applications [5–7]. In addition, due to the small wave number of this spectrum, mmWave devices have a small size [4]. Different frequency bands are licensed for 5G applications [6]. One of the challenges of designing a 5G antenna is that different countries have different licensed frequency bands. Frequency bands such as 24.75 GHz to 25.25 GHz, 27.5 GHz to 28.35 GHz, and 37 to 40 GHz are determined by the US Federal Communication Commission (FCC) as 5G bands. The 24.25 GHz to 27.5 GHz is licensed by the European telecommunications Standards Institute (ETSI) in Europe and the UK. 24.75 GHz to 27.5 GHz and 37 GHz to 42.5 GHz bands are planned for 5G applications by China. So a 5G antenna should cover two or more licensed bands. In addition to the new 5G applications, some other applications such as wearable antennas need to be updated. A new industrial, scientific, and medical (ISM) band including 24 GHz to 25 GHz is defined for 5G applications [8]. So designing a wearable antenna for this new ISM band is essential [8–10]. Wearable antennas are usually used in body area networks (BAN). Different applications are considered for wearable antennas including health monitoring, localization, etc. These antennas can be planted on clothes or Internet of Things (IoT) gadgets. As these antennas are planted on clothes, they may bended. It is essential for a wearable antenna to work properly in the case of bending conditions. The high number of design parameters of a 5G mmWave antenna makes it very challenging to design a 5G antenna. Machine learning approaches can help us to overcome this challenge [7, 11, 12]. However, machine learning approaches have high computational complexity. Using surrogate-based optimization (SBO) can reduce the computational complexity of these approaches [7]. SBO uses low-fidelity electromagnetic (EM) simulations instead of high-fidelity ones. Low-fidelity EM simulations are simulations with lower accuracy than high-fidelity ones.

* Corresponding author: Nazih Khaddaj Mallat (nazih.mallat@aau.ac.ae).
[1] College of Engineering, Al-Ain University, Al-Ain, UAE. [2] Department of Electrical Engineering, Sharif Unversity of Technology, Tehran, Iran. [3] Department of Elec. & Comp. Engineering, Tarbiat Modares, Tehran, Iran.

Various designs for 5G mmWave antennas are proposed in [1, 4, 7]. In [1], an mmWave microstrip antenna for 5G communications in 26 GHz resonance frequency is proposed. This antenna has 9 dB gain and 8.5 GHz bandwidth. This antenna has advantages such as high gain, wide bandwidth, and compact size. The bandwidth of this antenna covers the new ISM band. However, the substrate of this antenna is not flexible, and therefore this antenna is not suitable for IoT wearable applications. A broadband quasi Yagi-Uda antenna for 5G mmWave applications is proposed in [4]. This antenna has an 8.9 dB maximum realized gain and a 47% impedance bandwidth (IBW) in 28 GHz center frequency. The benefits of this antenna rely on its high gain and wide bandwidth. However, the radiation pattern of this antenna is not suitable for IoT applications. Furthermore, the dimension of this antenna is large too. A dual-band dual-polarized antenna for 5G mmWave systems is proposed in [7]. This antenna has a maximum gain of 9.4 dB. The impedance bandwidth of this antenna is 9% and 7.8% in 28 GHz and 38 GHz center frequencies, respectively. This antenna has high gain and suitable size for 5G applications. However, its bandwidth is small, and it does not cover the new ISM band.

Some different wearable antennas are proposed in [8–10]. A wearable antenna for the new ISM band is designed in [8]. This antenna has a 6 dB gain and an 800 MHz bandwidth. This antenna is fabricated on a flexible substrate (Rogers 6002). The authors tested the antenna under bending conditions. However, this antenna cannot cover other 5G bands such as 28 GHz and 38 GHz bands. Another wearable antenna with a textile substrate for the new ISM band is proposed in [9]. The maximum on-body gain of this antenna is 7 dB, and the bandwidth of this antenna is 10 GHz. However, the authors did not propose any experimental verification for this antenna. Authors in [10] proposed a wideband mmWave antenna for 5G applications based on PET substrate. The maximum gain of this antenna is 7.44 dB. Different learning approaches are proposed for the antenna optimization problem. In [3], the authors used the Kriging algorithm and LOLA-Voronoi sample selector to optimize the bandwidth and gain of a patch antenna. In [11], the authors proposed a multistage approach for multiobjective and multidimensional parameter spaces using Kriging methods. They used this approach to optimize the gain and bandwidth of a sub-6 antenna. In [12], an approach for antenna optimization based on accelerated gradient search is proposed. This approach is tested on three different antennas.

This paper is one of the first works which have used machine learning to design a wearable antenna for the new ISM band. In addition, the DDEA-SE approach used for optimization in this paper has not been used for antenna optimization before. The geometry of the antenna is novel, and it is not like other papers. In addition, unlike most of the ISM antennas, this antenna can cover ISM band and 5G band. Bending tests are performed, and the results of these tests are simulated.

2. WEARABLE ANTENNA DESIGN

To achieve a flexible antenna, a cotton substrate with $\epsilon_r = 1.6$ is used in the design of antenna. The design procedure starts with Ant. 1 which is a rectangular patch antenna. Fig. 1(a) shows this rectangular antenna. The response of this rectangular patch is shown in Fig. 3(a). This antenna has two operating bands in 15–40 GHz band. These operating bands are 15.3–16.4 GHz and 22.8–26.3 GHz frequencies. However, this antenna has no operating band in higher frequencies. To tune the impedance of higher frequencies, we changed the geometry of Ant. 1 and achieved Ant. 2. Fig. 1(a) shows Ant. 2. The return loss outcome of this antenna is shown in Fig. 3(a). Ant. 2 has four operating bands. These bands are 23.5–24.5 GHz, 25.2–26.6 GHz, 28.6–29.3 GHz, and 37.6–39.8 GHz. In fact, this subtraction decreases the electrical length of the antenna. This reduction of the electrical length creates resonance in higher frequencies. However, this change has an effect on lower operating bands and reduces the bandwidth of these operating bands. Fig. 1(b) shows the final design of the proposed antenna. To increase the bandwidth of the antenna and attain a multiband antenna, small triangles are removed from the onboard plane. This removing operation forms a fractal structure. The subtracted triangles dimension is $\frac{1}{9}$ of the onboard triangle. The spacing between these removed triangles is equal to 2.06 mm $(0.164\lambda_0$ at $f_0 = 24$ GHz). A simple plane forms the ground plane of this antenna. To achieve the desired bandwidth and gain, the other design parameters (w_1-w_3, l_1, and thickness of the substrate) should be tuned.
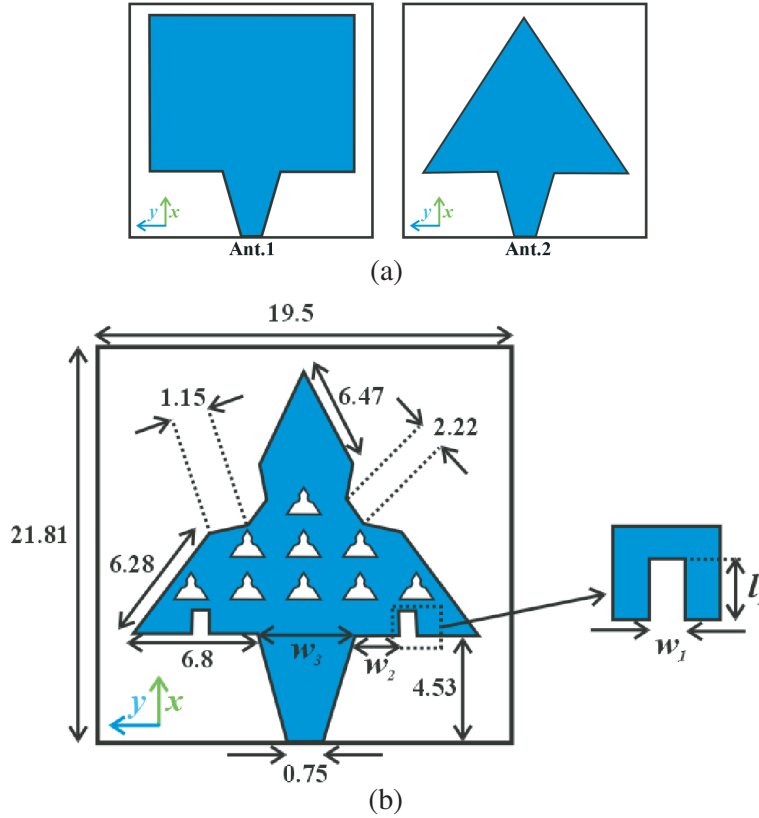
Figure 1. Geometry of the: (a) Ant. 1, Ant. 2 and (b) proposed antenna. All the values are in mm.

3. OPTIMIZATION PROCEDURE

To find the optimum value of the mentioned design parameters (w_1-w_3, l_1, and thickness of the substrate), an optimization procedure is utilized. The data-driven evolutionary algorithm using selective ensemble (DDEA-SE) proposed in [13] is used to perform this optimization. The vector of design variables is defined as follows:

$$\mathbf{x} = [w_1, w_2, w_3, l_1, h] \tag{1}$$

where h is the thickness of the substrate. The cost function of this optimization is defined as follows:

$$\mathfrak{F}(\mathbf{x}, f) = \sum_{i=1}^{N_{BW}} \left(\frac{1}{G_m^i(\mathbf{x}, f)} + \widetilde{S}_{11}^i(\mathbf{x}, f) \right) \tag{2}$$

where G_m^i and $\widetilde{S}_{11}^i$ are the maximum gain and mean of the return loss of the antenna in the ith desired band, respectively. It is clear that by increasing the maximum gain and decreasing the return loss (increasing the bandwidth) of the desired bands, the cost function defined by (2) will decrease.

One of the challenges of this optimization problem is the lack of a mathematical relation between (2) and components of (1). One of the solutions to this challenge is using model builders [3] and [13]. Model builders return a function that expresses the relationship between inputs and outputs of a database. In this paper, the proposed approach in [13], called DDEA-SE, is used as the optimization approach. The DDEA-SE uses a database to build surrogate models, and then by using a set of these surrogate models searches for the optimum points.

As our optimization problem is non-convex, several cases can fulfill our desired goals. We cannot stand that DDEA-SE can find the best optimum case, but it can find one of the optimum points ($\mathbf{x_{opt}}$) that fulfill our desired goals with good accuracy. To reduce the computational complexity of this

optimization problem, we used low-fidelity EM simulation to build the database. The low-fidelity EM simulations have a lesser accuracy and computational complexity than high-fidelity ones. Our database contains 2000 samples with components of $\mathbf{x}$ as the input and their corresponding value of F as outputs. These low-fidelity samples are achieved by HFSS software with a low resolution of meshes and a low number of passes. The high-fidelity simulation needs 10 passes while we used 6 passes in low-fidelity simulations. The mean time of each simulation is 190 seconds.

Simulations are performed in a computer with a Core i5 3.1 GHz CPU and 8 GB RAM. Our desired bands are 23 GHz to 26 GHz (covers ISM band and a part of China, FCC, and ETSI bands), 27.5 GHz to 28.5 GHz (covers FCC), and 35.5 GHz to 37.5 GHz (covers a part of FCC, China, and satellite bands). The optimization procedure is summarized as follows:

- First, a database based on low-fidelity EM simulations with design parameters (components of $\mathbf{x}$) as inputs and their corresponding F is collected using HFSS software.
- Then this database is given to DDEA-SE to build surrogate models of F based on $\mathbf{x}$.
- After that, DDEA-SE uses sets of these surrogate models to find one of the optimum points $\mathbf{x_{opt}}$.
- Then by means of HFSS software the result of optimization ($\mathbf{x_{opt}}$) is verified.

Figure 2 shows the block diagram of the optimization procedure, where x_i and F_i are the ith ($i \leq 2000$) input and output of the database. The output of this optimization procedure is $\mathbf{x_{opt}}$.

$$\mathbf{x_{opt}} = [0.5, \ 2.925, \ 2.65, \ 0.49, \ 0.5] \tag{3}$$
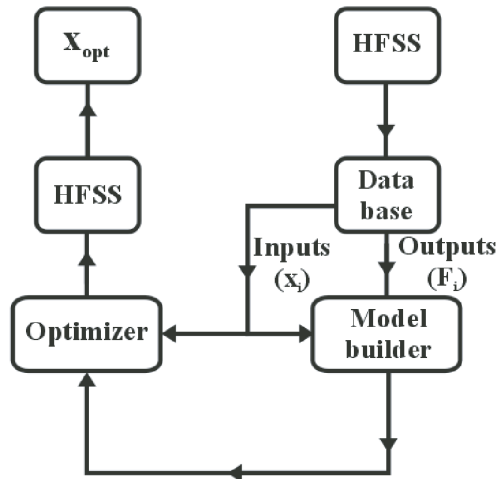

Figure 2. Block diagram of the optimization procedure.

3.1. Results of the Optimized Antenna

Figure 3 shows S_{11}, gain, and radiation pattern results of the optimized antenna. This antenna has three operation bandwidths in the range of 15 GHz to 40 GHz. Fig. 3(b) shows a resonance frequency near the 16 GHz with a bandwidth of 1.3 GHz, from 15.9 GHz to 17.2 GHz. The next one covers the 22.9 GHz to 25.9 GHz frequency band. This band contains the new ISM, FCC, ETSI, and China bands. This band includes our first desired band (23 GHz to 26 GHz) with 96% accuracy. The simulation result shows that the 27.64 GHz to 28.48 GHz band forms the third operation band. In contrast, in the measurement results, this band is not covered. This contrast is because of the use of low-fidelity EM solutions. The 35.5 GHz to 37.3 GHz band is the last operation band of this optimized antenna. This band covers our third desired band with 90% accuracy. A part of FCC and China bands are covered by this band. The total simulated gain of this antenna is 6.3 dB, 3.37 dB, and 4.6 dB in 24.5 GHz, 28 GHz, and 36 GHz frequencies, respectively. However, the measured gain of this antenna is 4 dB, 3.5 dB, and 4.1 dB in 24.5 GHz, 28 GHz, and 36 GHz frequencies, respectively. Fig. 3(b) shows the simulated and measured
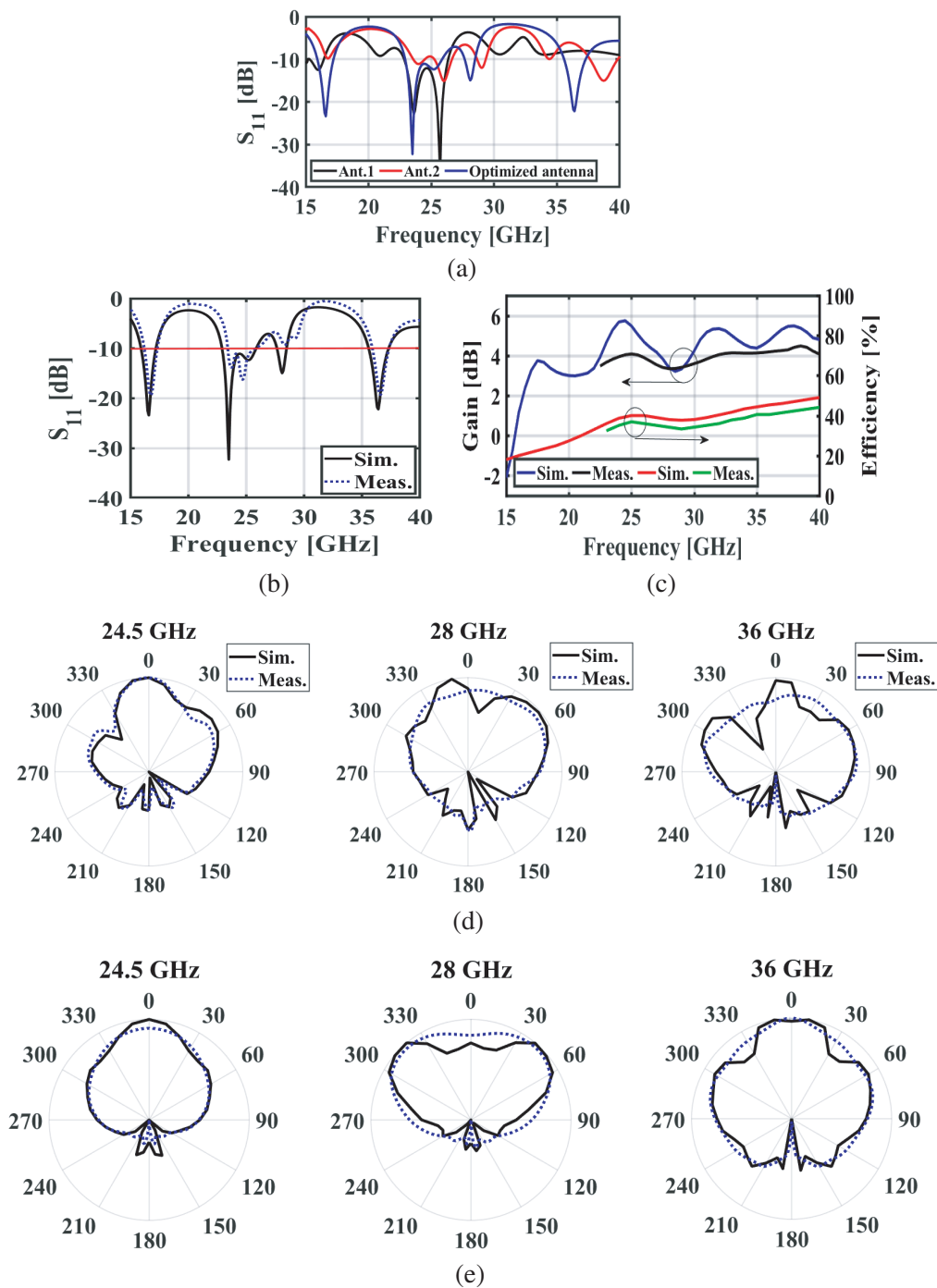
Figure 3. Results of the optimized antenna. (a) S_{11} of each step of design. (b) S_{11}. (c) Gain. (d) E-plane radiation pattern. (e) H-plane radiation pattern.

gains which shows appropriate adaptation with fabricated proposed antenna. The simulated efficiency of this antenna is shown in Fig. 3(c). This antenna has 40%, 37%, and 49% radiation efficiencies in 24.5 GHz, 28 GHz, and 36 GHz frequencies, respectively. The transmitting input power is set on 30 dBm, and the distance between Tx & Rx antennas is 2 m in an anechoic chamber.

Figures 3(d) and (e) show the E-plane and H-plane radiation patterns of the optimized antenna, respectively. The half-power beamwidth (HPBW) of this antenna in 24.5 GHz, 28 GHz, and 36 GHz

frequencies is 28°, 19.1°, and 15.3°, respectively. These amounts for H-plane are 46.19°, 45.65°, and 43° for 24.5 GHz, 28 GHz, and 36 GHz frequencies.

Table 1 provides a comparison between the proposed antenna and some other antennas. The number of bands of the proposed antenna is larger than the other compared papers. The antennas proposed in [8–10] and the proposed antenna are flexible, but [1] and [7] are not flexible. The antenna in [8] does not cover the 5G band. The antennas in [7] and [10] do not cover the new ISM band. However, the proposed antenna covers the new ISM band and a 5G band near 37 GHz. The effect of the bending is not mentioned in [9, 10], while we studied the effect of bending in our paper. The bandwidth of the proposed antenna is much higher than [8].

Table 1. Comparison table between the proposed antenna and some other antennas.

Design	f_0 (GHz)	max. G (dB)	No. bands	band width (GHz)	flexible	5G	ISM	bending test	max. G bending x	max. G bending y
[1]	26	9	1	8.5	×	✓	✓	×	-	-
[7]	28	9.4	2	1.7	×	✓	×	×	-	-
	38			3.2					-	-
[8]	24	6	1	0.8	✓	×	✓	✓	5.6	5.36
[9]	25	5.5	1	10	✓	✓	✓	×	-	-
[10]	28	7.44	1	14	✓	✓	×	×	-	-
proposed	16.5 24.5 36.5	4.5	3	1.3 3 1.8	✓	✓	✓	✓	4.9	3.48

4. ANTENNA PERFORMANCE UNDER BENDING CONDITIONS

Figure 4 demonstrates the antenna geometry under different bending angles. In Fig. 4(a), the antenna is bent over the x/y axis 90°. In most of the current works, antennas are tested under regular bending angles. In this paper, we test our antenna under an irregular bending angle according to Fig. 4(b). In this test, the antenna is bent over its diagonal 90°. Results of the bending tests are demonstrated in Fig. 5. Fig. 5(a) shows the return loss of the proposed antenna in these tests. The E-plane and H-plane radiation patterns of this antenna under these tests are shown in Figs. 5(b) and (c), respectively.
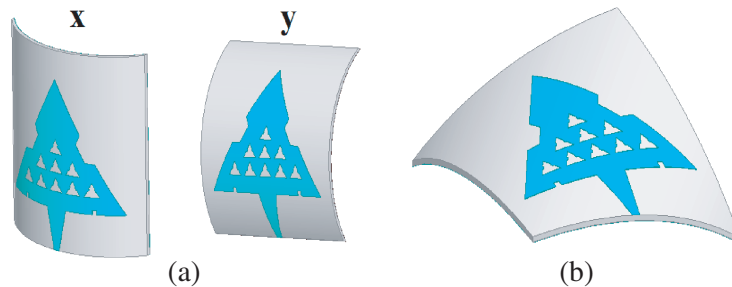

Figure 4. Antenna under bending conditions. (a) 90° over x or y axis. (b) 90° over x and y axis.

When this antenna is bent 90° over the x axis, it has five bandwidths in 15 GHz to 40 GHz including 15 GHz to 17.3 GHz, 22.37 GHz to 23.85 GHz, 24.26 GHz to 25.9 GHz, 26.85 GHz to 27.3 GHz, and 35 GHz to 37.36 GHz. The HPBW of this antenna on this condition in 24.5 GHz frequency is 60° and
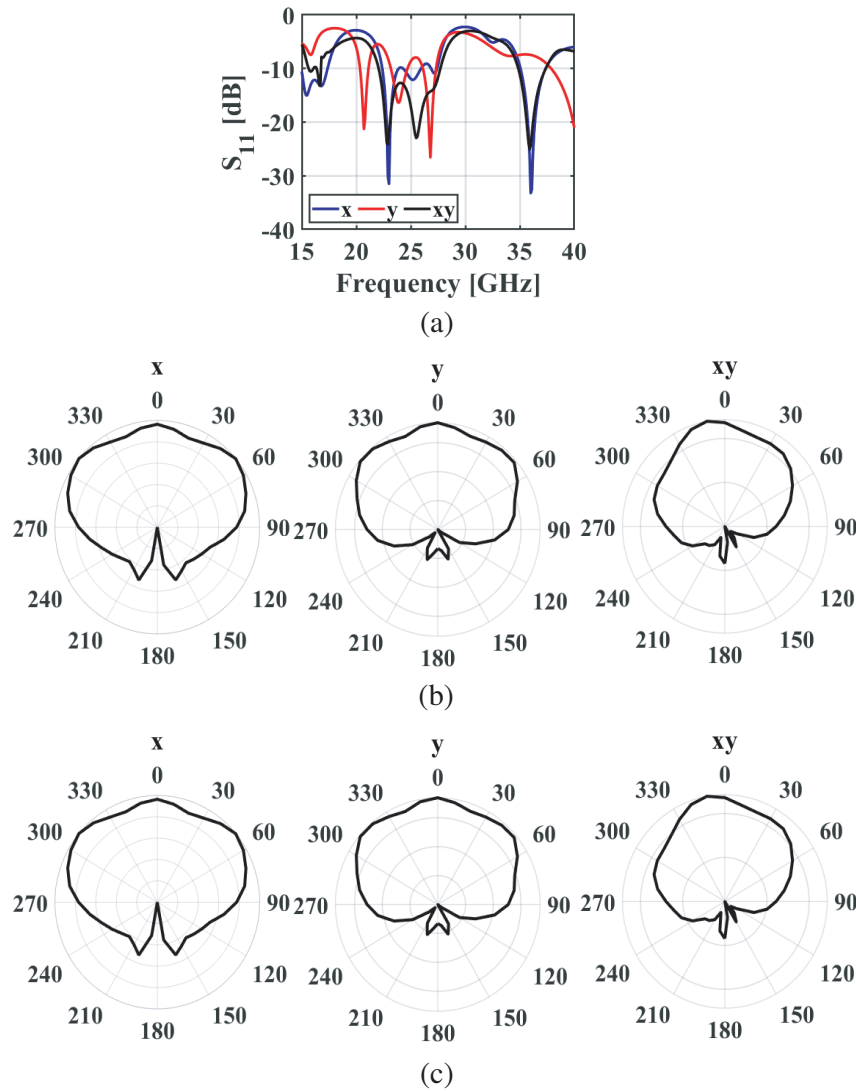
Figure 5. Simulation results of the optimized antenna under bending conditions. (a) S_{11} result. (b) E-plane radiation pattern in 24.5 GHz frequency. (c) H-plane radiation pattern in 24.5 GHz frequency.

$46°$ for E-plane and H-plane, respectively. The total gain of this antenna in this bending test is 4.9 dB. Results of bending antenna $90°$ over the y axis show that this antenna in this test has 4 bandwidths in the 15 GHz to 40 GHz frequency band. These bandwidths are 20.3 GHz to 21.09 GHz, 23.15 GHz to 24.65 GHz, 26.11 GHz to 27.11 GHz, and 37.87 to 40 GHz. This shows that the HPBW of this antenna in this bending angle is $78°$ and $135°$ for E-plane and H-plane in 24.5 GHz frequency, respectively. The maximum gain of this antenna is 3.48 dB. The third bending test, $90°$ over antenna diagonal, results in four bandwidths. 15.6 GHz to 16 GHz, 16.34 GHz to 16.75 GHz, 22 GHz to 27.7 GHz, and 34.8 GHz to 37.3 GHz are bandwidths of this antenna in this test. The HPBW of this antenna in this test and 24.5 GHz frequency is $34°$ and $73°$ for E-plane and H-plane, respectively. This antenna in this test has a 6.63 dB gain.

5. STUDY THE EFFECT OF THE DESIGN PARAMETERS

In this section, the effect of some design parameters on the antenna performance is studied. Fig. 6(a) shows the effect of the l_1 parameter on the return loss simulation results of the proposed antenna. This
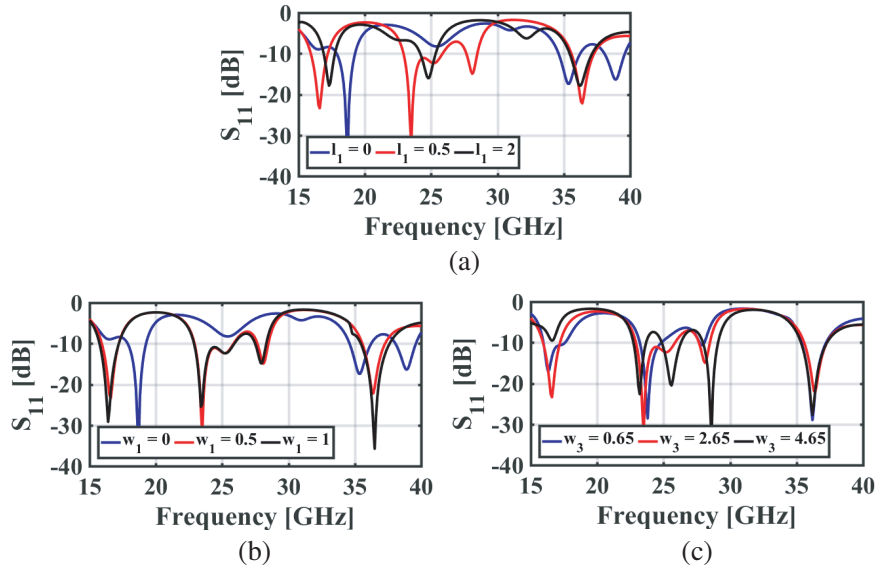
Figure 6. Performance results of the changing parameters in optimized antenna. (a) l_1, (b) w_1, (c) w_3.

parameter has a very high effect on the resonances of the antenna. The first resonance frequency of the antenna is moved by changing this parameter. The second and third resonance frequencies vanish when $l_1 = 0$. The higher resonance frequency of the antenna is changed by changing this parameter. Fig. 6(b) shows the influence of the w_1 on the return loss outcomes of the proposed antenna. This parameter has a big effect on second and third resonance frequencies. In addition, changing this parameter can change the first resonance frequency. The effect of w_3 is demonstrated in Fig. 6(c). By increasing w_3 we can add another resonance frequency near the 28 GHz frequency. However, by increasing this value, the first resonance lost its impedance match, and also the bandwidth of the second resonance frequency decreases.

6. CONCLUSION

In this paper, a multi-band flexible antenna is proposed for wearable and 5G applications. This antenna is fabricated on a cotton substrate. This arrow-shaped antenna has a fractal structure to achieve a multi-band antenna. To achieve the optimum value of the design parameters an optimization procedure based on the DDEA-SE algorithm is performed. This paper is one of the first attempts that try to design an ISM antenna using machine learning. This antenna not only covers the new ISM band, but also covers several 5G and satellite bands from 15 GHz to 40 GHz. To study the performance of this antenna as a wearable antenna, some bending tests are performed.

REFERENCES

1. Ozpinar, H., S. Aksimsek, and N. T. Tokan, "A novel compact, broadband, high gain millimeter-wave antenna for 5G beam steering applications," *IEEE Transactions on Vehicular Technology*, Vol. 69, No. 3, 2389–2397, 2020.
2. Choi, J., J. Park, Y. Youn, W. Hwang, H. Seong, Y. N. Whang, and W. Hong, "Frequency-adjustable planar folded slot antenna using fully integrated multithrow function for 5G mobile devices at millimeter-wave spectrum," *IEEE Transactions on Microwave Theory and Techniques*, Vol. 68, No. 5, 1872–1881, 2020.
3. Nouri, M., S. A. Aghdam, A. Jafarieh, N. K. Mallat, M. H. Jamaluddin, and M. Dor-Emami, "An optimized small compact rectangular antenna with meta-material based on fast multi-objective optimization for 5G mobile communication," *Journal of Computational Electronics*, 1–9, 2021.

4. Nouri, M., S. Abazari Aghdam, A. Jafarieh, J. Bagby, and S. Sahebghalam, "A wideband millimeter-wave antenna based on quasi Yagi antenna with MIMO circular array antenna beamforming for 5G wireless networks," *Microwave and Optical Technology Letters*, Vol. 61, No. 7, 1810–1814, 2019.

5. Mabrouk, I. B., M. Nedil, T. A. Denidni, and A. R. Sebak, "A novel design of radiation pattern-reconfigurable antenna system for millimeter-wave 5G applications," *IEEE Transactions on Antennas and Propagation*, Vol. 68, No. 4, 2585–2592, 2019.

6. Nouri, M., A. Jafarieh, H. Behroozi, N. K. Mallat, M. H. Jamaluddin, and S. A. Aghdam, "Compact 5G millimeter-wave dual-band filter with application in filtenna," *Microwave and Optical Technology Letters*, Vol. 63, No. 2, 620–625, 2021.

7. Mallat, N. K., M. Nouri, S. A. Aghdam, M. T. Zia, B. Harb, and A. Jafarieh, "A dual circularly reconfigurable polarization patch antenna for fifth generation mobile communication systems," *Progress In Electromagnetics Research C*, Vol. 105, 73–84, 2020.

8. Iqbal, A., A. Basir, A. Smida, N. K. Mallat, I. Elfergani, J. Rodriguez, and S. Kim, "Electromagnetic bandgap backed millimeter-wave MIMO antenna for wearable applications," *IEEE Access*, Vol. 7, 111135–111144, 2019.

9. Wagih, M., A. S. Weddell, and S. Beeby, "Millimeter-wave textile antenna for on-body RF energy harvesting in future 5G networks," *2019 IEEE Wireless Power Transfer Conference (WPTC)*, 245–248, IEEE, June 2019.

10. Jilani, S. F., Q. H. Abbasi, and A. Alomainy, "Inkjet-printed millimetre-wave PET-based flexible antenna for 5G wireless applications," *2018 IEEE MTT-S International Microwave Workshop Series on 5G Hardware and System Technologies (IMWS-5G)*, 1–3, IEEE, August 2018.

11. Jafarieh, A., M. Nouri, and H. Behroozi, "Optimized 5G-MMW compact Yagi-Uda antenna based on machine learning methodology," *2021 29th Iranian Conference on Electrical Engineering (ICEE)*, 751–756, IEEE, May 18, 2021.

12. Pietrenko Dabrowska, A. and S. Koziel, "Computationally efficient design optimisation of antennas by accelerated gradient search with sensitivity and design change monitoring," *IET Microwaves, Antennas & Propagation*, Vol. 14, No. 2, 165–170, 2020.

13. Wang, H., Y. Jin, C. Sun, and J. Doherty, "Offline data-driven evolutionary optimization using selective surrogate ensembles," *IEEE Transactions on Evolutionary Computation*, Vol. 23, No. 2, 203–216, 2018.